Identification of Residues Critical for the Interferon Antagonist Function of Langat Virus NS5 Reveals a Role for the RNA-Dependent RNA Polymerase Domain[▽]

Gregory S. Park,†‡ Keely L. Morris,† Roselyn G. Hallett, Marshall E. Bloom, and Sonja M. Best*

Laboratory of Persistent Viral Diseases, Rocky Mountain Laboratories, National Institute of Allergy and Infectious Diseases, Hamilton, Montana 59840

All pathogenic flaviviruses examined thus far inhibit host interferon (IFN) responses by suppressing the Janus kinase-signal transducer and activator of transcription (JAK-STAT) pathway. Both Langat virus (LGTV; a member of the tick-borne encephalitis virus serogroup) and Japanese encephalitis virus use the nonstructural protein NS5 to suppress JAK-STAT signaling. However, NS5 is also critical to virus replication, contributing methyltransferase and RNA-dependent RNA polymerase (RdRP) activities. The specific amino acid residues of NS5 involved in IFN antagonism are not known. Here, we demonstrate that the LGTV NS5 JAK-STAT inhibitory domain is contained between amino acids 355 and 735 (of 903), a range which lies within the RdRP domain. Furthermore, we identified two noncontiguous stretches of specific amino acids within the RdRP, 374 to 380 and 624 to 647, as critical for inhibition of JAK-STAT signaling. Despite considerable separation on the linear NS5 sequence, these residues localized adjacent to each other when modeled on the West Nile virus RdRP crystal structure. Due to the general conservation of RdRP structures, these results suggest that the specific residues identified act cooperatively to form a unique functional site on the RdRP responsible for JAK-STAT inhibition. This insight into the mechanism underlying flavivirus IFN evasion strategies will facilitate the design of antiviral therapeutics that potentiate the action of IFN during infection.

The flaviviruses cause globally significant human diseases and include tick-borne encephalitis (TBEV), dengue (DEN), Japanese encephalitis (JEV), West Nile (WNV), and yellow fever (YFV) viruses. There is currently no specific treatment for infection with any of these viruses, although interferon (IFN) has been trialed as a potential therapeutic (22, 25). IFN is a crucial element of the innate immune response to flavivirus infection, restricting virus replication, dissemination, and lethality in mouse models (1, 24). However, all flaviviruses examined thus far, including Langat virus (LGTV, a member of the TBEV serogroup) (2), JEV (14, 15), WNV (8), and DEN (10, 18), suppress IFN-mediated Janus kinase-signal transducer and activator of transcription (JAK-STAT) signal transduction (19). In response to stimulation with IFNs, these viruses compromise the phosphorylation, and hence activation, of JAKs, resulting in suppressed downstream signaling events, including STAT phosphorylation and nuclear translocation. It has recently been shown that the relative ability of WNV strains to suppress JAK-STAT signal transduction is a major virulence determinant (11). Thus, determining the precise mechanisms by which flaviviruses suppress IFN signaling is important to the understanding of flavivirus pathogenesis as well as to the development of novel antiviral therapeutics.

We previously demonstrated that LGTV utilizes its non-structural protein NS5 to inhibit IFN-mediated JAK-STAT signaling (2). Recently, JEV was also demonstrated to employ NS5 to suppress IFN-mediated JAK-STAT signaling (14). NS5 is the largest of the flavivirus nonstructural proteins at approximately 900 amino acids in length. It contributes two enzymatic domains required for RNA replication, the N-terminal S-adenosyl methionine-dependent methyltransferase (MTase) located between amino acids 1 and 296 (7, 23) and a C-terminal RNA-dependent RNA polymerase (RdRP) (12). RdRPs are defined by eight conserved motifs (I through VIII) (5, 12, 20) that, in LGTV NS5, occur between residues 456 and 735 and have an overall shape resembling a right hand with finger, palm, and thumb subdomains. Although the functions of NS5 in virus replication are relatively well characterized, the amino acid residues responsible for NS5-mediated antagonism of JAK-STAT signaling are not well defined.

In this report, we have defined the amino acid residues within LGTV NS5 required for its function as an IFN antagonist. We first examined the ability of various N- and C-terminal truncation constructs of NS5 to suppress the tyrosine phosphorylation of STAT1 (pY-STAT1) by flow cytometry analysis and immunofluorescence assay (IFA). The results demonstrated the minimal sequence of NS5 required for its IFN-inhibitory function to be amino acids 355 to 735, which map within the RdRP domain. We then further defined specific residues involved in IFN antagonism by using random and site-directed mutagenesis. These results demonstrated the presence of two noncontiguous sites within residues 355 to 735 requisite for the suppression of pY-STAT1. Together, these residues may form a unique functional site on the RdRP responsible for IFN antagonism.

* Corresponding author. Mailing address: Laboratory of Persistent Viral Diseases, Rocky Mountain Laboratories, National Institute of Allergy and Infectious Diseases, Hamilton, MT 59840. Phone: (406) 363-9284. Fax: (406) 363-9286. E-mail: sbest@niaid.nih.gov.
† These authors contributed equally to this work.
‡ Present address: University of Minnesota, Minneapolis, MN 55455.
▽ Published ahead of print on 25 April 2007.

TABLE 1. Primer sequences used to generate full-length and
N- and C-terminal truncations of LGTV NS5

Primer name	Sequence (5′ to 3′)[a]
LGT NS5 1F	*CACCATG*GGTGGATCCGAGGGAGAC
LGT NS5 221F	*CACCATG*TACTTCTCAACTGCCATCACGGGG
LGT NS5 342F	*CACCATG*GCAATGACTGACACAACTGC
LGT NS5 355F	*CACCATG*GTCTTTAAGGACAAAGTCG
LGT NS5 370F	*CACCATG*GGACCAAAATCATCATGAGAGC
LGT NS5 380F	*CACCATG*GACTGGCTGCTTGA
LGT NS5 457F	*CACCATG*ATGGGGAAAAGAGAGAAAAAGC
LGT NS5 456R	GTTGTACACACAATGGGCGCATCTCCCC
LGT NS5 684R	GTCATTGAGGAAGTAAAGGGCCTTGCTG
LGT NS5 731R	GTCACGGCACGGCACCAC
LGT NS5 735R	CAACTCATCCTGGTCACGGCACGGC
LGT NS5 847R	CAGGATGTCCTGTGATTTTGGCAG
LGT NS5 903R	AAATATTGAGCTCTCCAGTTTGAGCTC

[a] Bases in italics were added to the 5′ primers to facilitate cloning into the
TOPO Gateway system (Invitrogen).

TABLE 2. Primer sequences used to generate chimera NS5 cDNA
from LGTV and DEN4

Primer name	Sequence (5′ to 3′)[a]
DEN4 NS5 F	*CACCATG*GGAACTGGGACCACAGGAG AGACACTGGG
DEN4 NS5 R	CAGAACTCCTTCACTCTCTGAAGGAGC
DEN4 NS5 Msc1	GGTGGTAAAACTGCTAACA<u>TGGCCAT</u> GGGATGTGATTCCAATGG
LGT NS5 Mfe1 F	GCC<u>AATT</u>GGCTGCTTGAGCGAC
LGT NS5 Msc1 R	<u>TGGCCA</u>ACCCCAGAGTCCTC

[a] Bases in italics were added to the 5′ primers to facilitate cloning into the
TOPO Gateway system (Invitrogen). Underlined bases indicate engineered re-
striction endonuclease sites.

MATERIALS AND METHODS

Cloning and transfection. The LGTV E5 infectious cDNA clone provided by
A. Pletnev (National Institute of Allergy and Infectious Diseases [NIAID], NIH)
(4) served as a template for the cloning of LGTV NS5. DEN serotype 4 (DEN4)
NS5 was cloned from the DEN2 p4-1#3 infectious clone provided by S. White-
head (NIAID, NIH) (6). Each gene was PCR amplified and directionally cloned
into the Gateway entry vector, pENTR/SD/D-TOPO (Invitrogen, Carlsbad, CA),
followed by recombination into pcDNA6.2DEST/V5 (Invitrogen) to generate
C-terminal V5 epitope-tagged LGTV or DEN4 NS5 (2). C-terminal and N-
terminal truncation constructs were generated in the same way using LGTV NS5
in pcDNA6.2DEST/V5 as a template. All primers used for full-length and trun-
cated expression constructs are detailed in Tables 1 and 2. The sequence of each
construct was verified by DNA sequencing. Constructs were transfected into
Vero cells (ATCC, Manassas, VA) in six-well plates or in eight-well Labtek slides
(Fisher Scientific, Pittsburgh, PA) using Liptofectamine LTX and OptiMEM
(Invitrogen) according to the manufacturer's instructions. DNA constructs were
allowed to express for 24 h prior to the 15-min treatment with 1,000 U/ml of
recombinant human beta IFN (IFN-β) (R&D Systems, Minneapolis, MN).

To generate LGTV/DEN4 NS5 chimeras, LGTV NS5 cDNA was PCR am-
plified with a 5′ primer containing an MfeI site and a 3′ primer containing an
MscI site (Table 2) and ligated into the pCR2.1 (Invitrogen) cloning vector. The
resulting plasmid was digested with MfeI and MscI, followed by gel purification
of the insert and ligation into the similarly digested DEN4 NS5 cDNA (in
pENTR/SD/D-TOPO vector; using existing MfeI and MscI sites at nucleotides
1134 and 2335, respectively). To engineer the LGTV/DEN4 NS5 MscI-MscI
chimera, an additional MscI site was introduced into DEN4 NS5 cDNA by
site-directed mutagenesis at nucleotides 988 to 993 (Table 2), followed by diges-
tion with MscI. To obtain the compatible insert, a fragment of LGTV NS5 from
nucleotides 660 to 2334 was amplified by PCR with the same 3′ primer (see
above) containing the MscI site and the 5′ LGTV NS5 220F primer (Table 1) and
ligated into pCR2.1. This construct was digested with MscI to yield an insert
containing nucleotides 993 to 2334 that was then ligated into the modified DEN4
NS5 cDNA described above. LGTV/DEN4 NS5 MfeI-MscI and MscI-MscI
chimeras were confirmed by digestion and DNA sequencing in the pENTR/SD/
D-TOPO vector before recombination into pcDNA6.2DEST/V5 to generate
C-terminal V5 epitope-tagged chimeric constructs (see Fig. 2A). Expression in
Vero cells was confirmed by Western blotting and IFA using an anti-V5 mono-
clonal antibody.

Random and site-directed mutagenesis. The truncated LGTV NS5 sequence
representing amino acids 342 to 735 in pENTR/SD/D-TOPO was subjected to
random mutagenesis using a GeneMorph II EZclone Domain mutagenesis kit
(Stratagene, Cedar Creek, TX) with 100 ng of template DNA per reaction. The
resulting mutants were sequenced and recombined into pcDNA6.2DEST/V5 for
expression in Vero cells and testing of their ability to inhibit IFN-mediated
JAK-STAT signaling by IFA. Site-directed mutants were made using a
QuikChange XL site-directed mutagenesis kit according to the manufacturer's
instructions (Stratagene). Details of the mutational primer sequences can be
obtained from the authors. Mutants were confirmed by DNA sequencing, re-
combined into pcDNA6.2DEST/V5, expressed in Vero cells, and tested for their
ability to inhibit JAK-STAT signaling by IFA. Mutations conferring an altered
phenotype by IFA were introduced into full-length NS5 and tested by IFA and
flow cytometry.

Western blot analysis. Western blots on total cell lysates were performed as
previously described (2). The primary antibodies used were anti-V5 conjugated
to horseradish peroxidase (Invitrogen) at 1:5,000 and mouse anti-β-actin (Sigma,
St. Louis, MO) at 1:10,000. The secondary antibody used was horseradish per-
oxidase-conjugated goat anti-mouse (1:2,000; DAKO, Glostrup, Denmark).

Flow cytometry. Vero cells transfected with various NS5 expression constructs
were treated with IFN-β for 15 min, washed twice in cold Dulbecco's phosphate-
buffered saline and trypsinized for 10 min at 37°C to dislodge cells. Cells were
resuspended in freshly prepared 2% paraformaldehyde/Dulbecco's phosphate-
buffered saline and incubated for 10 min at 37°C, followed by permeabilization
in 90% methanol for 10 min on ice. The cells were washed once in stain buffer
(BD Pharmingen, San Diego, CA), followed by incubation with anti-pY(701)-
STAT1 conjugated to AlexaFluor 647 (BD Pharmingen) and anti-V5 conjugated
to fluorescein isothiocyanate (1:1,000; Invitrogen) for 45 min at room tempera-
ture in the dark. AlexaFluor 647- and fluorescein isothiocyanate-conjugated
mouse immunoglobulin G2a (IgG2a) were used as isotype controls. Cells were
washed once in stain buffer and analyzed using a FACSAria flow cytometer (BD
Biosciences) and FlowJo software, version 7.1 (Tree Star). After gating on
V5-positive cells, the percent pY-STAT1 inhibition was determined as the frac-
tion of V5-positive cells that were pY-STAT1 negative.

IFAs. Epitope-tagged NS5 protein expression and pY-STAT1 were examined
as previously described (2).

Sequence alignment and structural modeling. The amino acid sequences cor-
responding to NS5 from LGTV (GenBank accession no. AF253420), Western
TBEV (strain Hypr; GenBank accession no. AAB53095), JEV (RP-9; GenBank
accession no. AF014161), WNV (NY99-flamingo382-99; GenBank accession no.
AF196835), DEN4 (GenBank accession no. AY648301), DEN2 (GenBank ac-
cession no. NC_001474), and YFV (Asibi; GenBank accession no. AY640589)
were aligned using Clustal W alignment within DNAstar. The homologous amino
acids of LGTV important for JAK-STAT signaling were modeled on the WNV
NS5 structure (Protein Data Bank code 2HFZ) (17) using PyMol.

Statistical analysis. Data from flow cytometry was analyzed by analysis of
variance (ANOVA) with Tukey's posttest to determine significant differences
($P < 0.05$) between individual groups.

RESULTS

**Identification of the domain within NS5 required for JAK-
STAT antagonism.** Our previous results demonstrated that
expression of LGTV NS5 in the absence of other viral proteins
prevented the accumulation of pY-STAT1 in response to
IFN-β (2). To determine the subregion of LGTV NS5 required
for this antagonism of IFN-mediated JAK-STAT signaling, a
series of N- and C-terminally truncated LGTV NS5 expression
constructs were made, each in frame with a C-terminal V5
epitope tag (Fig. 1A). These constructs were transfected into
Vero cells, and their expression and expected molecular mass
were verified by Western blotting (Fig. 1B).

To test the ability of each NS5 construct to impede JAK-STAT
signaling, flow cytometry was performed with permeabilized,
IFN-β-stimulated Vero cells expressing each V5-fusion protein
using antibodies that recognize pY-STAT1 and V5. The use of
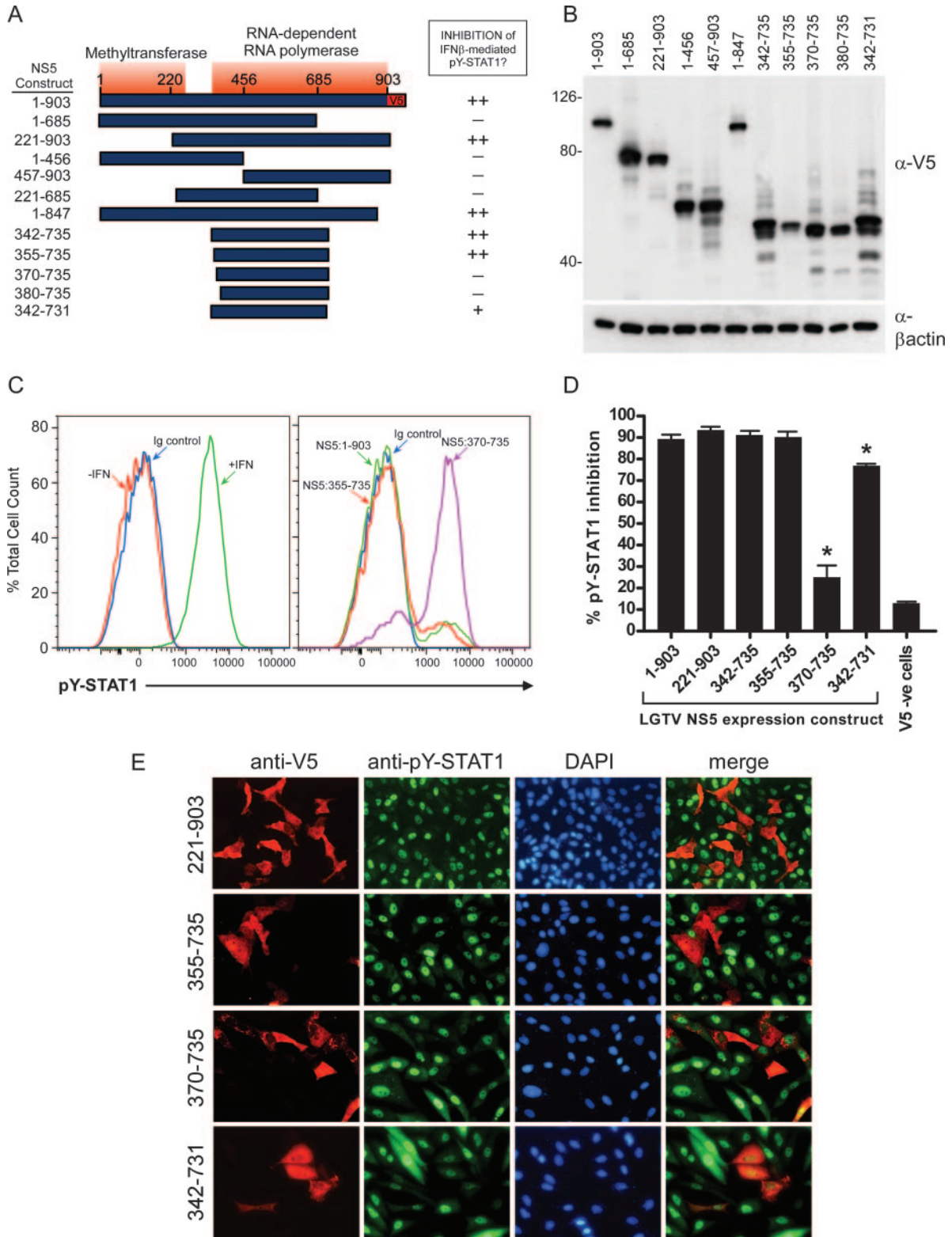flow cytometry to measure the phosphorylation status of STAT1

FIG. 1. Identification of the LGTV NS5 JAK-STAT inhibitory domain. (A) Schematic summarizing full-length (1-to-903) and truncated LGTV NS5 expression constructs and their ability to prevent nuclear accumulation of pY-STAT1 in response to IFN-β. All constructs were expressed in frame with a C-terminal V5 epitope tag. MTase and RdRP domains are indicated in red. (B) Western blot probed for the V5 epitope tag, demonstrating the expression and relative size of each NS5 construct in Vero cells. Approximate molecular mass (in kilodaltons) is indicated. (C) Flow cytometry to determine the percent inhibition of pY-STAT1 in Vero cells transfected with LGTV NS5-derived expression constructs. The left panel shows pY-STAT1 levels in permeabilized Vero cells. Examples of untreated cells (−IFN; red), cells treated with IFN-β (+IFN; green) and IFN-β-treated cells expressing LGTV NS5 and stained with an IgG2a-AlexaFluor 647 isotype (Ig control; blue) are shown. The right panel

provides advantages over other measurements, including IFA, due to its quantitative output, as well as gene-reporter assays, because the transfection efficiency between samples can be normalized by gating on V5-positive cells. The percent pY-STAT1 inhibition for each protein was defined as the proportion of V5-expressing cells that were pY-STAT1 negative. Staining of pY-STAT1 in transfected and control cells and staining of isotype controls are shown in Fig. 1C.

Following systematic removal of 25% or 50% of the NS5 coding sequence (the five clones represented in Fig. 1A, 1-685 to 221-685), only the expression of the NS5 construct from residues 221 to 903 (NS5:221-903) retained a wild-type (WT) phenotype in which approximately 90% of V5-positive cells were pY-STAT1 negative (Fig. 1A and D). We found that NS5 expression constructs progressively truncated from the C terminus to residue 735 retained a WT phenotype of inhibition (Fig. 1D, NS5:342-735 and NS5:355-735). However, the removal of an additional four C-terminal amino acids to residue 731 significantly reduced the ability of NS5 to inhibit IFN-mediated JAK-STAT signal transduction (Fig. 1D). The N terminus of LGTV NS5 could be truncated as far as amino acid 355 and still retain the WT phenotype in this assay (Fig. 1C and D). However, additional N-terminal truncation of LGTV NS5 to residue 370 resulted in a construct with a mutant phenotype, in that pY-STAT1 was present in the majority of NS5:370-735-expressing cells treated with IFN-β (Fig. 1C and D). The results obtained by flow cytometry were confirmed visually using IFA (Fig. 1E). Vero cells expressing NS5:221-903 or NS5:355-735 were generally negative for pY-STAT1, whereas cells expressing NS5:370-735 or NS5:342-731 contained measurable pY-STAT1. Together, these studies suggested that the minimal linear sequence of NS5 required for WT inhibition of JAK-STAT signaling was contained within residues 355 to 735. Strikingly, this region overlaps with the finger region and the eight conserved motifs of the LGTV RdRP (shown in detail in Fig. 4), suggesting that the RdRP domain has a central role in IFN antagonism.

Construction of DEN4/LGTV NS5 chimeras. The minimal linear sequence of LGTV NS5 (NS5:355-735) required for a WT phenotype of JAK-STAT antagonism is 380 amino acids in length. It is possible that the strict sequence requirement for this function is actually shorter, with truncation to less than NS5:355-735 resulting in structural instability and loss of function. To address this issue, we wanted to express the inhibitory domain in the context of a full-length NS5 molecule. DEN NS5 is not an efficient inhibitor of JAK-STAT signaling (18) but is approximately 40% identical to LGTV NS5 at the amino acid level and has a similar predicted secondary structure. Hence, we constructed two NS5 chimeras between the LGTV and DEN4 NS5 molecules in an attempt to transfer the LGTV JAK-STAT inhibitory domain to DEN4 NS5. The two chimeric constructs contained DEN4 NS5 as the backbone with the central region derived from LGTV NS5 (Fig. 2A). The C-terminal LGTV NS5/DEN4 NS5 border was kept constant in both chimeras, occurring at amino acids 778 to 779. The N-terminal border of LGTV NS5 was bounded either at residues 379 to 380 (DEN4/LGTV NS5 MfeI-MscI) or at residue 332 (DEN4/LGTV NS5 MscI-MscI). Only the latter chimera encompassed the entire LGTV NS5 inhibitory domain identified above (residues 355 to 735).

Following expression in Vero cells and treatment with IFN-β, the ability of each protein to prevent nuclear accumulation of pY-STAT1 was examined by flow cytometry and IFA (Fig. 2B and C). As expected, DEN4 NS5 did not efficiently inhibit JAK-STAT signal transduction in Vero cells compared to LGTV NS5. However, expression of the DEN4/LGTV NS5 MscI-MscI chimera resulted in suppression of both phosphorylation (Fig. 2B) and nuclear localization (Fig. 2C) of STAT1, similar to that observed following expression of full-length LGTV NS5. In contrast, DEN4/LGTV NS5 MfeI-MscI containing the shorter LGTV sequence was not significantly different from WT DEN4 NS5 (Fig. 2B). Thus, incorporation of the LGTV NS5 JAK-STAT inhibitory domain into DEN4 NS5 is sufficient to render the chimeric protein an efficient inhibitor of JAK-STAT signaling. These results suggest that the mutant phenotype of inhibition associated with truncation of the N terminus beyond amino acid 355 is due to removal of residues involved in the suppression of signaling and is not due simply to structural instability of those proteins. Furthermore, these results suggest that LGTV-specific amino acids that are essential for JAK-STAT antagonism exist between amino acids 355 and 380.

Random and site-directed mutagenesis of LGTV NS5:342-735. To further explore the critical sequence requirements for antagonism of IFN responses, NS5:342-735 cDNA was subjected to random mutagenesis such that each clone generated contained an average of between one and four coding changes. A total of 288 clones were transfected into Vero cells and screened for their ability to inhibit IFN-mediated JAK-STAT signaling by IFA. The criterion in the initial IFA for stating that a mutant had an altered ability to prevent JAK-STAT signaling was that detectable nuclear pY-STAT1 was present in at least 20% of V5-positive cells. The sequence of each clone was also determined, which indicated that, collectively, these clones represented changes in ~66% of the amino acid sequence.

The precise clone information for the random mutants is depicted in Fig. 3A. Each individual clone demonstrating a
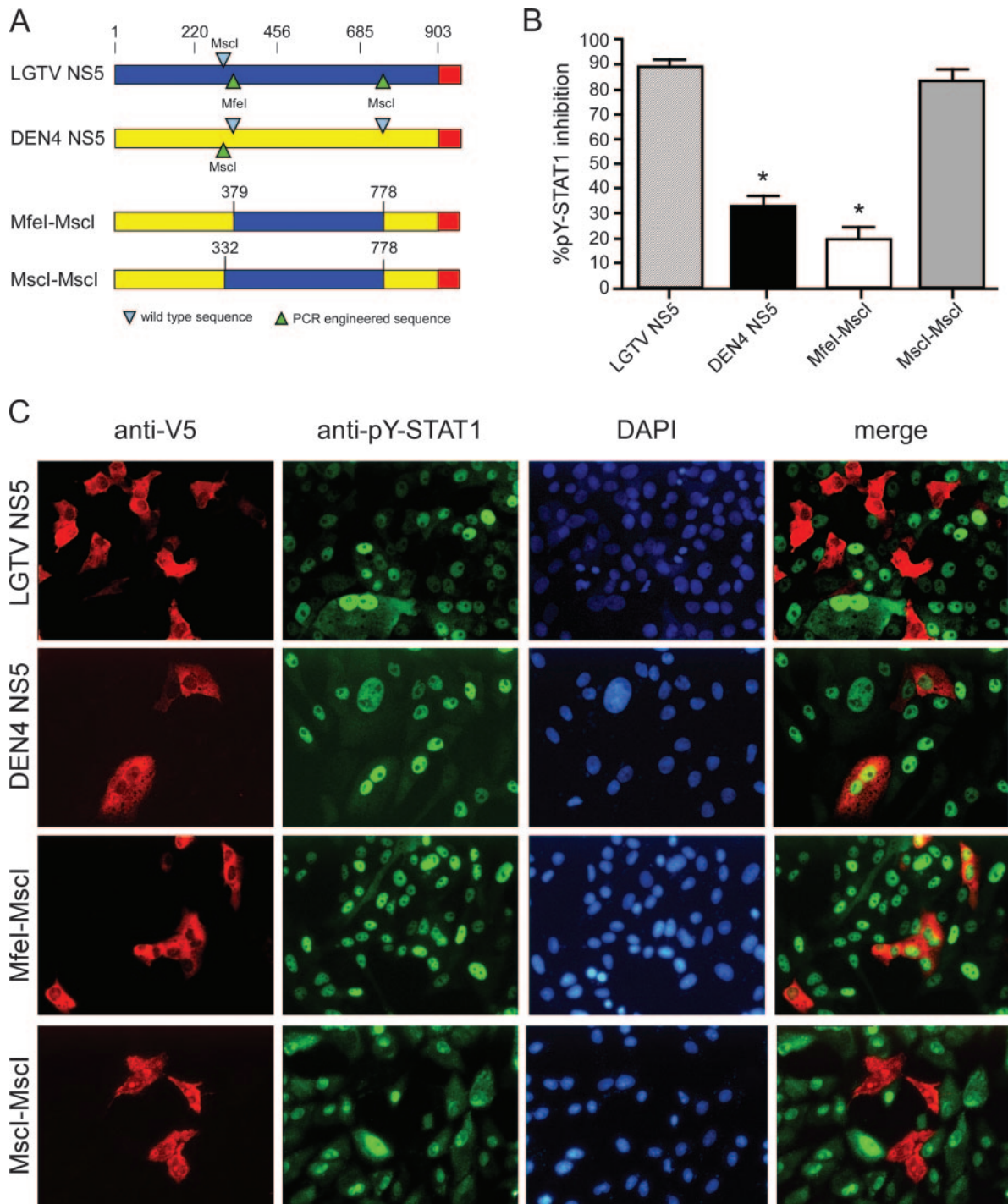
FIG. 2. LGTV and DEN4 NS5 chimeras. (A) Schematic of the two chimeras using DEN4 NS5 (yellow) as the backbone and containing central portions derived from LGTV NS5 (blue). Each was constructed in frame with a C-terminal V5 epitope tag (red). Restriction sites utilized to construct the Mfe1-Msc1 and Msc1-MscI chimeric NS5 molecules are indicated. (B) Quantification of pY-STAT1 inhibition by each construct analyzed by flow cytometry. Error bars indicate SEM; asterisks indicate significant differences from LGTV NS5 ($P < 0.05$ by ANOVA followed by Tukey's test). (C) IFA of WT LGTV NS5, WT DEN4 NS5, and chimeric Mfe1-Msc1 and Msc1-MscI NS5 proteins. Vero cells expressing each construct were treated with IFN-β and stained for the V5 epitope tag (red) and phosphorylated STAT1 (pY-STAT1; green) and counterstained with DAPI (blue) to show the cell nucleus.

mutant phenotype of JAK-STAT signaling by IFA is listed at the bottom of the table. The number of amino acid substitutions in each clone compared to the WT sequence is represented as 1 (red), 2 (blue), 3 (yellow), 4 (green) or 5 or more

(assorted colors) amino acids. Clones that retained a WT phenotype by IFA are not depicted individually. Instead, the coding changes found in all of these clones are represented as light pink boxes.
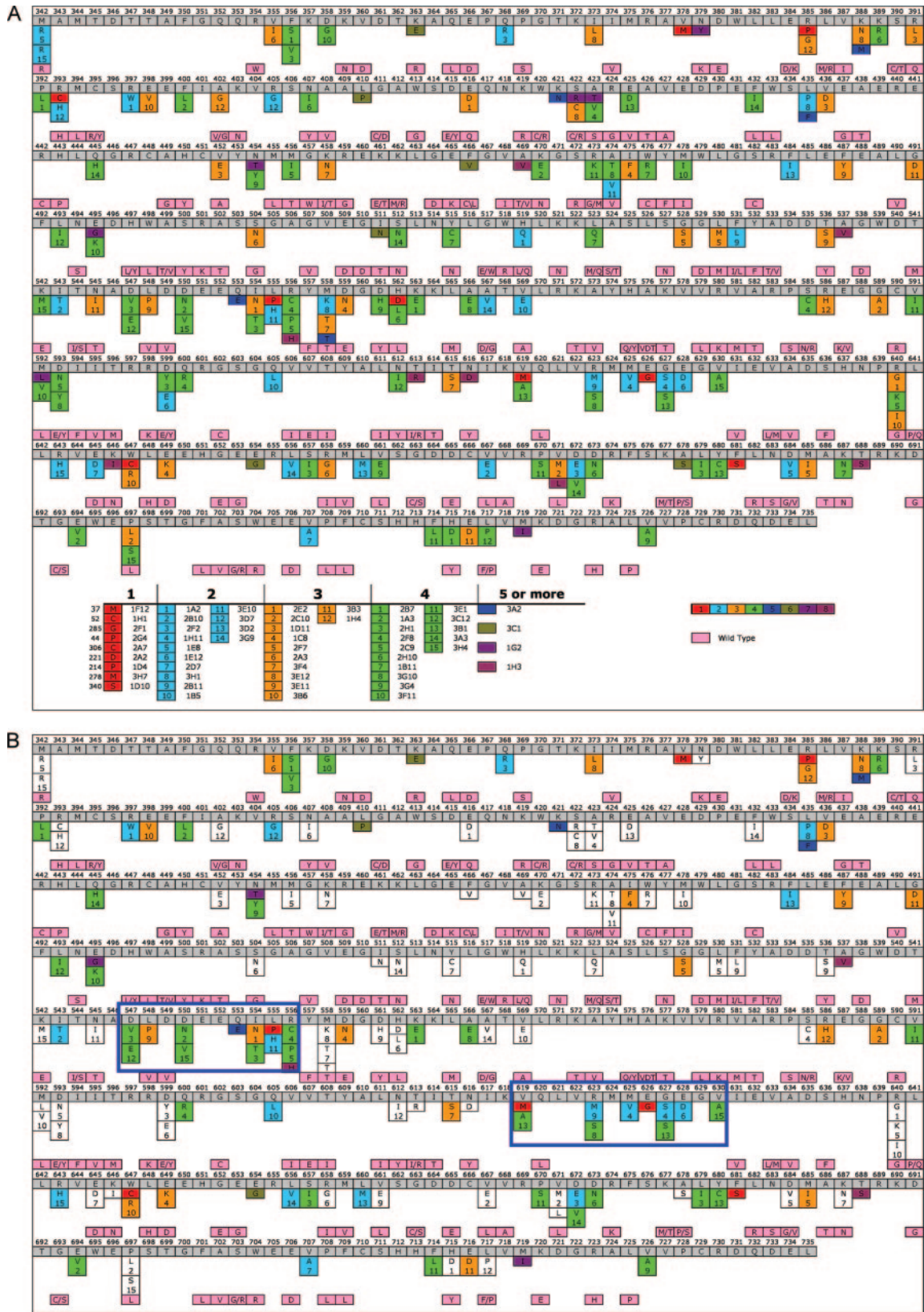
FIG. 3. Coding changes within LGTV NS5:342-735 following random mutagenesis and their association with a WT or mutant phenotype of JAK-STAT inhibition. (A) Each individual clone demonstrating a mutant phenotype (V5 and pY-STAT1 double-positive cells) by IFA is represented as containing 1 (red), 2 (blue), 3 (yellow), 4 (green), or 5 or more (assorted colors) amino acid changes compared to the WT sequence. Coding changes in clones that retained a WT phenotype by IFA are represented in light pink. See the text for an example of the use of this table. (B) Summary of the comparison of clones exhibiting WT and mutant phenotypes by IFA from Fig. 3A. Amino acid substitutions present in both WT and mutant clones were considered unlikely to significantly contribute to IFN antagonism and are represented in white. Residues that could not be ruled out using this process of elimination retain their original color coding. This left two predominant areas of NS5 that may directly contribute to IFN antagonism (large open blue boxes).

As an example of how to use the tables in Fig. 3, take clone number 11 in blue (clone 3E10) listed at the bottom of Fig. 3A. The expression of this clone exhibited a mutant phenotype of pY-STAT1 inhibition and contained two amino acid substitutions at A474V and L555H (the substitutions in clone 3E10 are represented in blue under the respective WT amino acid; these blue boxes also contain the number 11, referring to blue clone 11). However, the coding change at A474V was also found in a clone exhibiting a WT phenotype of JAK-STAT inhibition (represented in light pink), suggesting that A474 does not significantly contribute to the function of the IFN antagonist domain and that L555 may have a role. We worked our way through all clones using this process of elimination, which is summarized in Fig. 3B. In this table, residues thought not to contribute to IFN antagonism, including A474, are represented in white, while those that could not be ruled out retain their original color coding. Using this process of elimination, two predominant areas of NS5 that may directly contribute to IFN antagonism were identified; these are between residues 547 and 556 and between residues 619 and 630 (Fig. 3B, large open blue boxes).

Based on this information and the results from the LGTV/DEN4 NS5 chimeras, individual residues were chosen for site-directed mutagenesis to Ala (A). However, if the LGTV NS5 sequence at that residue coded for an Ala, the residue was then mutated to the corresponding residue of the DEN4 NS5 sequence. In addition to the substitutions suggested by the random mutagenesis studies, site-directed mutations were made to ablate potential functional sites in LGTV NS5:342-735. These included mutations at predicted phosphorylation sites (3), as well as a ^{663}GDD^{665}-to-^{663}GAA^{665} double mutant to disrupt the RdRP active site (16, 20). All site-directed mutants were again expressed in Vero cells and examined for their ability to inhibit JAK-STAT signaling by IFA. Important mutations in NS5:342-735 were subsequently introduced into full-length LGTV NS5 to confirm their importance in the context of the entire molecule by flow cytometry.

The summary of the site-directed mutagenesis studies is presented in Fig. 4A. A total of 53 unique site-directed mutant clones of LGTV NS5:342-735 were examined by IFA. Those mutants that retained a WT phenotype of inhibition are demonstrated by yellow boxes in Fig. 4A, whereas those that exhibited a mutant phenotype are represented in red. Examples of the ability of selected site-directed mutants of NS5:342-735 to inhibit IFN-β-mediated pY-STAT1 by IFA are shown in Fig. 4B.

Initially, three noncontiguous stretches of amino acids were demonstrated as important for the function of LGTV NS5 as an antagonist of IFN signal transduction (Fig. 4A). The first stretch lay between amino acids 374 and 380, with R376 and D380 determined to be critical since their mutation to Ala reduced the ability of full-length NS5 to prevent nuclear accumulation of pY-STAT1 by at least 60% (Fig. 4C). These residues lie within the most N-terminal portion (amino acids 355 to 380) of the LGTV NS5 domain responsible for JAK-STAT inhibition, as determined both by N-terminal truncation and by the DEN4/LGTV NS5 chimeras.

The second area of importance consisted of two residues examined in the context of a double mutation, LR555/556AA. However, while NS5:342-735 containing the LR555/556AA double mutation displayed a marked change in the phenotype of pY-STAT1 by IFA (Fig. 4B), the introduction of this mutation into full-length NS5 resulted in a WT phenotype by flow cytometry (Fig. 4C). This result suggests that LR555/556AA affects the JAK-STAT antagonist domain when expressed in isolation from the remainder of NS5 but has minimal influence on this function in the context of full-length NS5.

The third stretch of residues implicated in JAK-STAT inhibition lay between amino acids 624 and 647. The full-length NS5 mutant containing VI630/631AA exhibited poor expression and thus was not included in the analysis by flow cytometry. However, full-length NS5 constructs containing mutations at E626, E628, and W647 had at least a 60% reduction in their ability to inhibit JAK-STAT signaling (Fig. 4C).

These mutagenesis studies also defined residues within the RdRP that were not involved in JAK-STAT antagonism (Fig. 4A, yellow boxes). Most notably, the RdRP active site double mutant (DD664/665AA) retained a WT phenotype of inhibition (Fig. 4B and C). Residues predicted to be phosphorylated at S390, S396, S422, S504, T536, T544, S585, S636, Y680, T688, T692, and S703 were shown by either random (Fig. 3B) or site-directed mutagenesis (Fig. 4A) not to be critical to NS5-mediated inhibition of JAK-STAT signaling. These studies did not address the role of five additional predicted phosphorylation sites, namely, T362, S414, S503, S657, and S662.

Structural modeling of homologous *Flaviviridae* RdRPs. The atomic structures of RdRP domains from two closely related flaviviruses, WNV and DEN, have recently been reported (17, 26). To further understand the potential of residues identified as critical for NS5-mediated antagonism of JAK-STAT signaling, we aligned the LGTV NS5 protein sequence with those from WNV, DEN2, and DEN4 as well as TBEV, JEV, and YFV (Fig. 5A to C). The homologous amino acids of interest based on the mutagenesis studies were then modeled on the WNV RdRP three-dimensional structure (Fig. 5D), which is approximately 63% identical at the amino acid level to that of the LGTV RdRP domain.

The residues identified as important in the N terminus of the JAK-STAT inhibitory domain (374 to 380; IMR. . .D) (Fig. 5D) lie within an alpha helix of the WNV finger subdomain. The second residue cluster (624 to 647; M.E.E.VIX$_{15}$W) (Fig. 5D) originates toward the end of an alpha helix and extends into a loop structure and a second alpha helix of the palm subdomain. Despite the substantial linear distance (250 amino acids) between the two amino acid stretches identified by mutagenesis, the two regions model proximal to each other, on the lower outer left of the WNV RdRP structure. While the residues LR555/556 also modeled in the same general region of the RdRP (Fig. 5D), they appear not to contribute to the same pocket occupied by the other residues of interest on the RdRP domain. This potentially explains their minimal contribution to inhibition in the context of full-length NS5. Taken together, the results from the homologous RdRP model and the ability to inhibit pY-STAT1 in the context of full-length NS5 suggest that LGTV NS5:374-380 and NS5:624-647 act cooperatively on the LGTV RdRP structure to suppress IFN-stimulated JAK-STAT signaling.
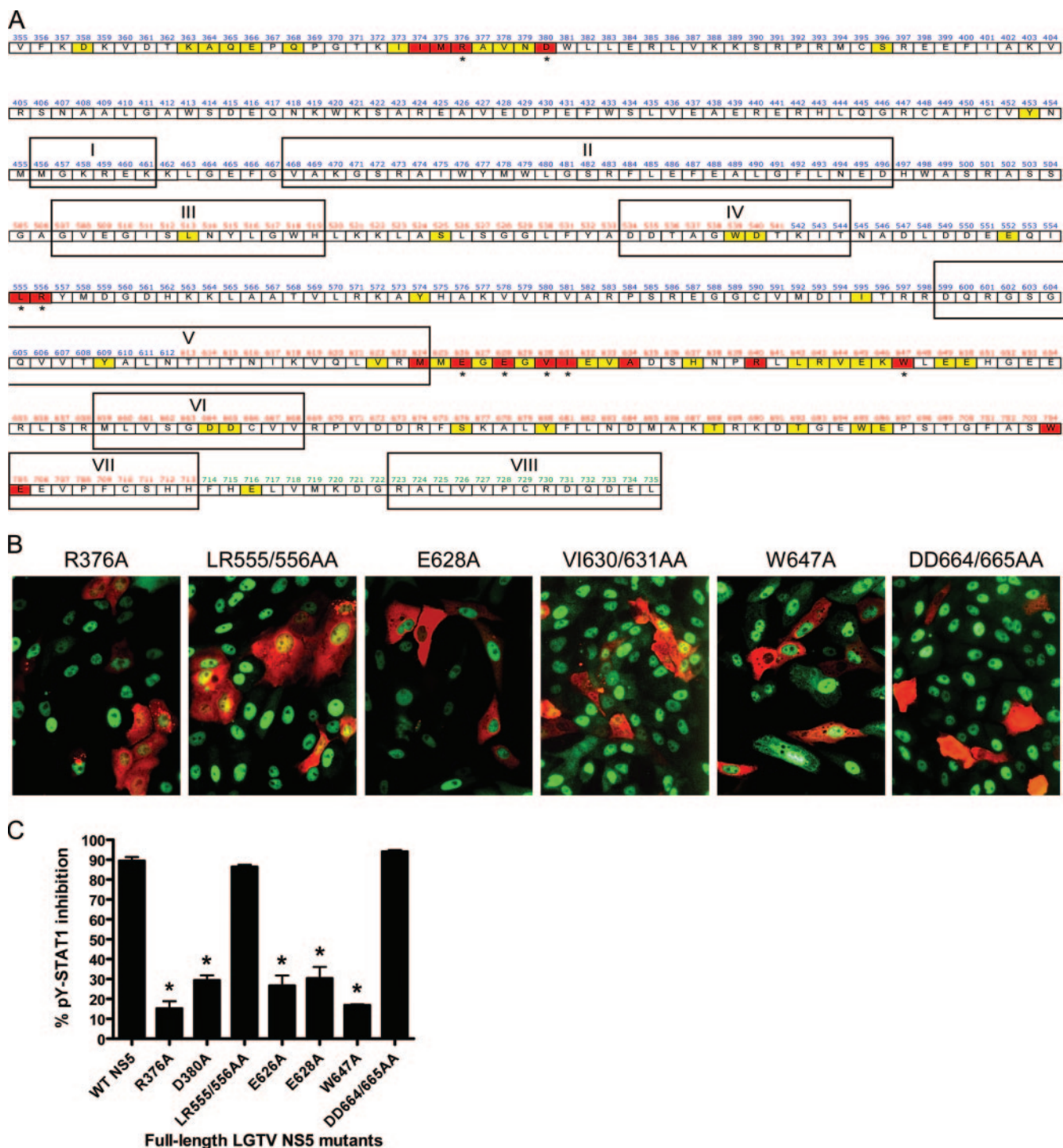
FIG. 4. Identification of critical residues within LGTV NS5:355-735 required for JAK-STAT inhibition. (A) Summary of site-directed mutations made in NS5:342-735. The number of each amino acid within the RdRP is indicated in blue (finger subdomain), red (palm subdomain), or green (thumb subdomain). The eight conserved RdRP motifs within LGTV NS5 are boxed (I through VIII). Amino acids represented in yellow indicate site-directed substitutions to Ala that resulted in a WT phenotype of pY-STAT1 inhibition by IFA. Those marked in red indicate site-directed substitutions to Ala that resulted in a mutant phenotype of pY-STAT1 inhibition by IFA. An asterisk indicates a strong change in phenotype, with approximately 80% of V5-positive cells containing nuclear pY-STAT1. Red boxes without an underlying asterisk indicate a moderate change in phenotype, with approximately 20 to 50% V5 positive cells also containing detectable pY-STAT1. (B) IFA of select site-directed mutants of LGTV NS5:342-735. Vero cells expressing each construct were treated with IFN-β and stained for the V5 epitope tag (red) and phosphorylated STAT1 (pY-STAT1; green). The DD664/665AA mutant exhibited a WT phenotype of inhibition, whereas all others depicted here had a mutant phenotype. (C) Quantification of pY-STAT1 inhibition by each full-length NS5 construct analyzed by flow cytometry. Error bars indicate SEM; asterisks indicate significant differences from WT LGTV NS5 ($P < 0.05$ by ANOVA followed by Tukey's test).

A

```
         * * *       *
LGTV  369 PGTKIIMRAVNDWLLERLVKKS 390
WTBEV 369 PGTRVIMRAVNDWILERLAQKS 390
JEV   370 AGAKEVLNETTNWLWAYLSREK 391
WNV   370 EGVKYVLNETTNWLWAFLAREK 391
DEN4  368 PGTRMVMTTTANWLWALLGKKK 389
DEN2  368 EGTKKLMKITAEWLWKELGKKK 389
YFV   369 AGTRKIMKVVNRWLFRHLAREK 390
```

B

```
             * *
LGTV  550 DEEQILRYMDGDHKK 564
WTBEV 550 DEEQILRYMEGEHKQ 564
JEV   551 NEAKVLELLDGEHRM 565
WNV   551 NEAKVLELLDGEHRR 565
DEN4  549 NEELITEQMAPHHKI 562
DEN2  549 NEEMITNHMAGEHKK 562
YFV   550 DEQEILNYMSPHHKK 564
```

C

```
          * *  *  * *         *    *
LGTV  620 QLVRMMEGEVIEVADSHNPR---LLRVEKWLEEHGEERLSRMLVSGDDCVV 668
WTBEV 620 QLVRMMEGEVIEAADAHNPR---LLRVERWLKEHGEERLGRMLVSGDDCVV 668
JEV   621 QLVRLMEAEGVIGPQHLEQLPRKNKIAVRTWLFENGEERVTRMAISGDDCVV 672
WNV   621 QLVRMMEGEGVIGPDDVEKLTKGKGPKVRTWLFENGEERLSRMAVSGDDCVV 672
DEN4  618 QLIRQMEAEGVITQDDMQNPKG-LKERVEKWLKECGVDRLKRMAISGDDCVV 668
DEN2  618 QLIRQMEGEGIFKSIQHLTAS--EEIAVQDWLARVGRERLSRMAISGDDCVV 667
YFV   620 QLIRMAEAEMVIHHQHVQDCDESVLTRLEAWLTEHGCNRLKRMAVSGDDCVV 671
```
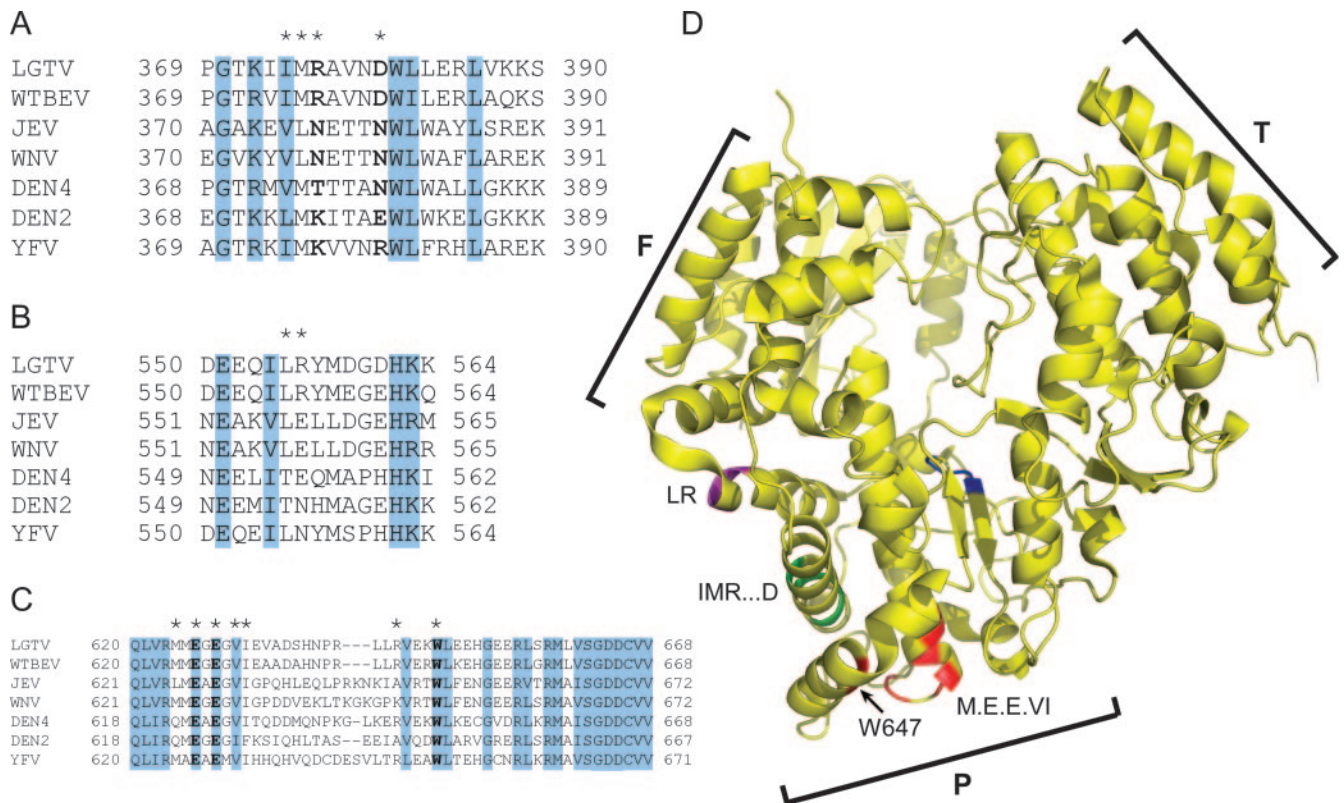
D

FIG. 5. Alignment of critical residues within the LGTV NS5 JAK-STAT inhibitory domain with related flaviviruses. LGTV NS5 was aligned with NS5 from TBEV (Western subtype, strain Hypr; WTBEV), JEV, WNV, DEN4 and DEN2, and YFV. Alignments highlighting regions surrounding LGTV (A) NS5:374-380, (B) NS5 LR555/556, and (C) NS5:624-647 are shown. Residues in LGTV NS5 demonstrated as important for its function in JAK-STAT inhibition are indicated with an asterisk, with critical residues as demonstrated by flow cytometry indicated in boldface type. Residues strictly conserved throughout the vector-borne flaviviruses are shaded in blue. (D) Model of aligned LGTV NS5 residues important for JAK-STAT inhibition on the WNV RdRP structure. LGTV NS5 residues 374 to 380 (IMR. . .D; green), LR555/556 (LR; pink), and 624 to 647 (M.E.E.VIX$_{15}$W [M.E.E.VI]; red) and the GDD active site (blue) are shown. The RdRP finger (F), palm (P), and thumb (T) subdomains are indicated.

DISCUSSION

The NS5 protein of both LGTV and JEV mediates multiple indispensable and distinct functions during replication. The RdRP and MTase domains are obligatory for RNA replication, whereas a third domain confers resistance to IFN via inhibition of JAK-STAT signal transduction (2, 14). The structure and function of the RdRP and MTase are relatively well characterized, although the domain responsible for JAK-STAT inhibition was largely unknown. In this work, we first identified the linear domain within LGTV NS5 responsible for JAK-STAT inhibition as residing between amino acid residues 355 and 735 (Fig. 1). This domain overlaps precisely with conserved features of the RdRP, namely the finger region and the eight conserved RdRP motifs (Fig. 4). The superimposition of the JAK-STAT inhibitory domain within the RdRP suggests an inextricable evolutionary relationship between RNA replication and IFN resistance.

By analyzing an extensive panel of mutants, we further refined the specific amino acids critical for the function of NS5 as a suppressor of IFN-mediated signaling. These residues clustered in two short, noncontiguous stretches of amino acids within the JAK-STAT inhibitory domain. The first of these, residues 374 to 380, resides within the RdRP finger domain,

whereas residues 624 to 647 belong to the RdRP palm domain. Despite their significant separation on the linear NS5 sequence, the two amino acid groups localize adjacent to one another when modeled on the crystal structure of the WNV RdRP (17) (Fig. 5). Taken together, these results strongly suggest that the specific amino acids identified by mutagenesis contribute to a unique functional site on the polymerase responsible for the disruption of JAK-STAT signaling.

The IFN antagonist function of the RdRP did not appear to depend upon key motifs necessary for RdRP activity. Each of the eight conserved motifs within the *Flaviviridae* RdRP contain residues involved in RNA replication, functioning in template binding (motif II), binding catalytic ions (motif VI, which contains the RdRP active site, GDD), and GTP or NTP binding (motifs I, III, IV, V, VII, and VIII) (5). Conserved residues within each motif are obligatory for HCV RdRP activity (16, 20) or contribute to the GTP binding site of BVDV RdRP (5). In the course of our studies, mutation of many conserved residues critical for GTP or NTP binding in motifs I (for LGTV NS5, M456 and K458), II (R473), IV (D540), V (T608 and N612), and VI (DD664/665) had no effect on NS5-mediated inhibition of JAK-STAT signaling (Fig. 3A and 4A). Notably, the DD664/665AA site-directed double mutant of

LGTV NS5 should be incapable of RdRP activity (9, 13, 16, 20), but this mutation had no effect on nuclear accumulation of pY-STAT1. Thus, while the IFN-antagonist function of NS5 will certainly be affected by structural alterations in the RdRP, neither the RdRP active site nor an intact GTP binding site are required. However, the RdRP activity of LGTV NS5 containing specific mutations in 374 to 380 and 624 to 647 must be tested to determine if polymerase activity and JAK-STAT inhibition are strictly independent.

The precise mechanism of JAK-STAT inhibition by NS5 is not known. In the current study, four of the five mutant expression constructs exhibiting a strong change in the phenotype of pY-STAT1 inhibition contained substitutions for charged residues (R376, D380, E626, and E628), which would be expected to reside on the surface of NS5. Hence, these residues are potential mediators of the protein-protein interactions involved in the suppression of JAK-STAT signal transduction. We previously identified an association between LGTV and IFN receptor complexes (2) and are currently working to determine if this association is affected by key mutations in NS5. The finding that the C-terminal border of the LGTV NS5 JAK-STAT antagonist domain occurs near residue 735 is consistent with work by Lin et al. whereby the IFN antagonist function of JEV NS5 was not affected by C-terminal truncation to residue 762 but was compromised following further truncation to residue 667 (14). However, in contrast to our results, N-terminal deletion of the first 84 or 167 residues of JEV NS5 abrogated its function as an IFN antagonist. Despite these differences between studies, it remains possible that the JAK-STAT inhibitory domains in LGTV and JEV are similarly located in the proteins. A simple explanation of the differences between studies is that the N-terminal deletion series we made in LGTV NS5 were more structurally favorable and retained the nascent properties of the protein.

Inhibition of JAK phosphorylation by JEV NS5 was associated with protein tyrosine phosphatase (PTP) activity (14). Significant PTPs involved in the normal negative regulation of JAK-STAT signal transduction include Src homology 2 (SH2) domain containing tyrosine phosphatase 1 (SHP-1) and SHP-2, PTP1B/T-cell PTP, and CD45. Specific inhibition of PTP1B and CD45 did not restore the IFN antagonist activity of JEV NS5 (14). SHP activation requires substrate recognition of phosphorylated tyrosine residues (21). We mutated every tyrosine residue within LGTV NS5:355-735 by random or site-directed mutagenesis with no effect on IFN-stimulated nuclear accumulation of pY-STAT1. Hence, it is unlikely that phosphorylated tyrosines within NS5 serve as substrates to directly activate SHPs. However, indirect activation of these phosphatases by NS5 may occur, such as through the activation of additional kinases that positively regulate PTPs. Alternatively, noncanonical PTPs may also be invoked. Importantly, although JAK-STAT signaling is regulated via a series of tyrosine phosphorylation events, our results suggest that NS5's function as a JAK-STAT antagonist is not itself directly mediated by tyrosine phosphorylation.

Results from the LGTV/DEN4 chimeras suggested that LGTV-specific residues exist in the N terminus of the JAK-STAT inhibitory domain and are important for the suppression of pY-STAT1. We found two LGTV NS5 residues, R376 and D380, that were both critical for inhibition and different from the corresponding DEN4 sequence, thus potentially contributing to this virus-specific function of NS5. However, an examination of protein sequences from the broader group of vector-borne viruses showed that these two residues are similar between LGTV and DEN2 NS5 yet different between LGTV and JEV NS5 (Fig. 5A). Furthermore, the second cluster of LGTV NS5 residues critical for inhibiting JAK-STAT signaling is highly conserved among the vector-borne flaviviruses (Fig. 5C). Since our results do not identify unique amino acids that correlate with the viruses that utilize NS5 as their predominant JAK-STAT antagonist (14, 18), additional residues are likely to influence IFN antagonism. Furthermore, structural deviations between the various flavivirus RdRPs may also determine NS5's competence to suppress IFN responses. The recently determined atomic structure of RdRP domains from WNV and DEN (17, 26) can be used to predict, and thus more precisely define, residues involved in the suppression of IFN signaling. This work will provide further insight into the immune evasion strategies utilized by these highly pathogenic viruses. Identification of the specific RdRP residues responsible for the antagonism of IFN responses is an important first step in the development of therapeutics aimed at disrupting this critical aspect of virus pathogenesis.

REFERENCES

1. **Best, S. M., D. N. Mitzel, and M. E. Bloom.** 2006. Action and reaction: the arthropod-borne flaviviruses and host interferon responses. Future Virol. **1:**447–459.
2. **Best, S. M., K. L. Morris, J. G. Shannon, S. J. Robertson, D. N. Mitzel, G. S. Park, E. Boer, J. B. Wolfinbarger, and M. E. Bloom.** 2005. Inhibition of interferon-stimulated JAK-STAT signaling by a tick-borne flavivirus and identification of NS5 as an interferon antagonist. J. Virol. **79:**12828–12839.
3. **Blom, N., S. Gammeltoft, and S. Brunak.** 1999. Sequence and structure-based prediction of eukaryotic protein phosphorylation sites. J. Mol. Biol. **294:**1351–1362.
4. **Campbell, M. S., and A. G. Pletnev.** 2000. Infectious cDNA clones of Langat tick-borne flavivirus that differ from their parent in peripheral neurovirulence. Virology **269:**225–237.
5. **Choi, K. H., J. M. Groarke, D. C. Young, R. J. Kuhn, J. L. Smith, D. C. Pevear, and M. G. Rossmann.** 2004. The structure of the RNA-dependent RNA polymerase from bovine viral diarrhea virus establishes the role of GTP in de novo initiation. Proc. Natl. Acad. Sci. USA **101:**4425–4430.
6. **Durbin, A. P., R. A. Karron, W. Sun, D. W. Vaughn, M. J. Reynolds, J. R. Perreault, B. Thumar, R. Men, C. J. Lai, W. R. Elkins, R. M. Chanock, B. R. Murphy, and S. S. Whitehead.** 2001. Attenuation and immunogenicity in humans of a live dengue virus type-4 vaccine candidate with a 30 nucleotide deletion in its 3'-untranslated region. Am. J. Trop. Med. Hyg. **65:**405–413.
7. **Egloff, M. P., D. Benarroch, B. Selisko, J. L. Romette, and B. Canard.** 2002. An RNA cap (nucleoside-2'-O-)-methyltransferase in the flavivirus RNA polymerase NS5: crystal structure and functional characterization. EMBO J. **21:**2757–2768.
8. **Guo, J. T., J. Hayashi, and C. Seeger.** 2005. West Nile virus inhibits the signal transduction pathway of alpha interferon. J. Virol. **79:**1343–1350.
9. **Guyatt, K. J., E. G. Westaway, and A. A. Khromykh.** 2001. Expression and purification of enzymatically active recombinant RNA-dependent RNA polymerase (NS5) of the flavivirus Kunjin. J. Virol. Methods **92:**37–44.
10. **Ho, L. J., L. F. Hung, C. Y. Weng, W. L. Wu, P. Chou, Y. L. Lin, D. M. Chang, T. Y. Tai, and J. H. Lai.** 2005. Dengue virus type 2 antagonizes IFN-alpha but not IFN-gamma antiviral effect via down-regulating Tyk2-STAT signaling in the human dendritic cell. J. Immunol. **174:**8163–8172.

11. **Keller, B. C., B. L. Fredericksen, M. A. Samuel, R. E. Mock, P. W. Mason, M. S. Diamond, and M. Gale, Jr.** 2006. Resistance to alpha/beta interferon is a determinant of West Nile virus replication fitness and virulence. J. Virol. **80:**9424–9434.

12. **Koonin, E. V.** 1991. The phylogeny of RNA-dependent RNA polymerases of positive-strand RNA viruses. J. Gen. Virol. **72:**2197–2206.

13. **Lai, V. C., C. C. Kao, E. Ferrari, J. Park, A. S. Uss, J. Wright-Minogue, Z. Hong, and J. Y. Lau.** 1999. Mutational analysis of bovine viral diarrhea virus RNA-dependent RNA polymerase. J. Virol. **73:**10129–10136.

14. **Lin, R. J., B. L. Chang, H. P. Yu, C. L. Liao, and Y. L. Lin.** 2006. Blocking of interferon-induced Jak-Stat signaling by Japanese encephalitis virus NS5 through a protein tyrosine phosphatase-mediated mechanism. J. Virol. **80:**5908–5918.

15. **Lin, R. J., C. L. Liao, E. Lin, and Y. L. Lin.** 2004. Blocking of the alpha interferon-induced Jak-Stat signaling pathway by Japanese encephalitis virus infection. J. Virol. **78:**9285–9294.

16. **Lohmann, V., F. Korner, U. Herian, and R. Bartenschlager.** 1997. Biochemical properties of hepatitis C virus NS5B RNA-dependent RNA polymerase and identification of amino acid sequence motifs essential for enzymatic activity. J. Virol. **71:**8416–8428.

17. **Malet, H., M. P. Egloff, B. Selisko, R. E. Butcher, P. J. Wright, M. Roberts, A. Gruez, G. Sulzenbacher, C. Vonrhein, G. Bricogne, J. M. Mackenzie, A. A. Khromykh, A. D. Davidson, and B. Canard.** 2007. Crystal structure of the RNA polymerase domain of the West Nile virus non-structural protein 5. J. Biol. Chem. **282:**10678–10689.

18. **Munoz-Jordan, J. L., G. G. Sanchez-Burgos, M. Laurent-Rolle, and A. Garcia-Sastre.** 2003. Inhibition of interferon signaling by dengue virus. Proc. Natl. Acad. Sci. USA **100:**14333–14338.

19. **Platanias, L. C.** 2005. Mechanisms of type-I- and type-II-interferon-mediated signalling. Nat. Rev. Immunol. **5:**375–386.

20. **Poch, O., I. Sauvaget, M. Delarue, and N. Tordo.** 1989. Identification of four conserved motifs among the RNA-dependent polymerase encoding elements. EMBO J. **8:**3867–3874.

21. **Poole, A. W., and M. L. Jones.** 2005. A SHPing tale: perspectives on the regulation of SHP-1 and SHP-2 tyrosine phosphatases by the C-terminal tail. Cell. Signal. **17:**1323–1332.

22. **Rahal, J. J., J. Anderson, C. Rosenberg, T. Reagan, and L. L. Thompson.** 2004. Effect of interferon-alpha2b therapy on St. Louis viral meningoencephalitis: clinical and laboratory results of a pilot study. J. Infect. Dis. **190:**1084–1087.

23. **Ray, D., A. Shah, M. Tilgner, Y. Guo, Y. Zhao, H. Dong, T. S. Deas, Y. Zhou, H. Li, and P. Y. Shi.** 2006. West Nile virus 5′-cap structure is formed by sequential guanine N-7 and ribose 2′-O methylations by nonstructural protein 5. J. Virol. **80:**8362–8370.

24. **Samuel, M. A., and M. S. Diamond.** 2006. Pathogenesis of West Nile virus infection: a balance between virulence, innate and adaptive immunity, and viral evasion. J. Virol. **80:**9349–9360.

25. **Solomon, T., N. M. Dung, B. Wills, R. Kneen, M. Gainsborough, T. V. Diet, T. T. Thuy, H. T. Loan, V. C. Khanh, D. W. Vaughn, N. J. White, and J. J. Farrar.** 2003. Interferon alfa-2a in Japanese encephalitis: a randomised double-blind placebo-controlled trial. Lancet **361:**821–826.

26. **Yap, T. L., T. Xu, Y.-L. Chen, H. Malet, M.-P. Egloff, B. Canard, S. G. Vasudevan, and J. Lescar.** 2007. Crystal structure of the dengue virus RNA-dependent RNA polymerase catalytic domain at 1.85-angstrom resolution. J. Virol. **81:**4753–4765.